

A Multilevel Sampling Algorithm for Locating Inhomogeneous Media

Keji Liu* Jun Zou[†]

July 8, 2018

Abstract

In the reconstruction process of unknown multiple scattering objects in inverse medium scattering problems, the first important step is to effectively locate some approximate domains that contain all inhomogeneous media. Without such an effective step, one may have to take a much larger computational domain than actually needed in the reconstruction of all scattering objects, thus resulting in a huge additional computational efforts. In this work we propose a simple and efficient multilevel reconstruction algorithm to help locate an accurate position and shape of each inhomogeneous medium. Then other existing effective but computationally more demanding reconstruction algorithms may be applied in these initially located computational domains to achieve more accurate shapes of the scatter and the contrast values over each medium domain. The new algorithm exhibits several strengths: robustness against noise, requiring less incidences, fast convergence, flexibility to deal with scatterers of special shapes, and advantages in computational complexity.

Key Words. Inverse medium scattering, initialization, multilevel reconstruction.

MSC classifications. 35R30, 65N20, 78A46.

1 Introduction

This work investigates the numerical identification of inhomogeneous medium scatterers by scattered fields. The inverse scattering problem can find wide applications in medicine, geophysics, biological studies. A large variety of numerical reconstruction

*Department of Mathematics, The Chinese University of Hong Kong, Shatin, Hong Kong. (kjliu@math.cuhk.edu.hk)

[†]Department of Mathematics, The Chinese University of Hong Kong, Shatin, Hong Kong. The work of this author was substantially supported by Hong Kong RGC grants (Projects 405110 and 404611). (zou@math.cuhk.edu.hk)

methods are available in literature, such as the time-reversal multiple signal classification (MUSIC) method [8, 14], the contrast source inversion (CSI) method [16, 17, 1], the continuation method [2], the subspace-based optimization method (SBOM) [4, 5], the linear sampling or probing methods (LSM) [6, 15, 11], the parallel radial bisection method (PRBM) [13], etc. In order to carry out any of these methods for the reconstruction of unknown multiple scattering objects, the first important step is to effectively locate some approximate domains that contain all scattering objects. Without such an effective step, one may have to take a much larger computational domain than actually needed in the reconstruction of all scattering objects. In particular, when multiple separated objects are present, and at least two of them are far away from each other, then one may need to set an initial sampling or computational domain to be much larger in order to ensure a safe covering of all such objects. One may easily have an initial computational domain with an area or a volume of 30 or 40 times as large as the actual region required to cover all unknown inhomogeneous medium objects. A much larger computational domain results usually in a huge additional computational effort for the entire numerical reconstruction process, considering the severe ill-posedness and strong nonlinearity of inverse medium scattering problems.

So it is of great significance for the reconstruction process of an inverse medium problem to have an effective step that helps locate the initial regions that cover each of the scattering object. In addition, this first step should be less expensive computationally and easy to implement numerically. It is mostly challenging to realize this target, and to provide an acceptable initial location of each scattering object at the same time. A direct sampling method was proposed recently in [7] for the purpose. The algorithm is computationally very cheap as it involves computing only the inner product of the scattered field with fundamental solutions located at sampling points. In this work, we will propose a new algorithm for the purpose, and it is completely different from the one in [7]. This new algorithm is an iterative one, also very cheap; only three matrix-vector multiplications are needed at each iteration, without any matrix inversion or solutions of linear systems involved. Most interestingly, the algorithm can first separate all disjoint objects quickly, usually in a few iterations, then refine its approximation successively and finally provide a good approximate domain for each separate object.

It is worth mentioning that the multilevel algorithm to be presented here is essentially different in nature from the multilevel linear sampling method developed in [11]: the new method is much less sensitive to the so-called cut-off values, it works with much less incident fields, and it does not need to solve ill-posed far-field equations at sampling points. In addition, the new algorithm is robust in the presence of noise and less sensitive to the noise level. More importantly, unlike most existing methods, the new method does not involve any optimization process or matrix inversions, so it can be viewed as a direct sampling method. Another nice feature of the new algorithm is that it is self-adaptive, that is, at each iteration it can remedy the possible errors from the previous iterations. With an effective initial location of each object, we may then apply any existing efficient but computationally more demanding methods, e.g., the methods in [2] [5] [17], for further refinement of the estimated shape of each scattering object as well as for recovery of the

contrast profiles of different media.

2 Problem description

Consider an inverse scattering problem where the scatterer Ω , possibly consisting of several separated disjoint components, is located in a homogeneous background medium \mathbb{R}^d ($d = 2, 3$). We assume that the scattered obstacles are illuminated successively by a number of plane wave incident fields $u_j^{inc}(\mathbf{x})$, $j = 1, 2, \dots, N_i$. For each plane wave incidence, the scattered field $u^{sca}(\mathbf{x}_q^s)$ is measured by the receivers at locations $\mathbf{x}_1^s, \dots, \mathbf{x}_{N_s}^s$; see Figure 1 for the incidences and receivers located on a circle S .

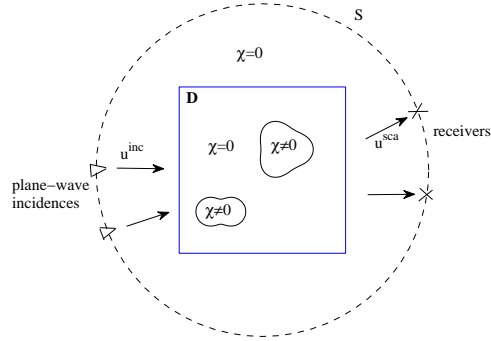


Figure 1: Geometrical model of the scattering problem.

The inverse scattering problem is to determine the contrast function or index of refraction, $\chi(\mathbf{x})$ for any point \mathbf{x} varying in the scatterer Ω , given a set of $N_i N_s$ scattering data u^{sca} . The contrast χ has a very important property, namely it vanishes outside the scattering obstacles. For each incident field, the total field u_j satisfies the Helmholtz equation [6]:

$$\Delta u_j(\mathbf{x}) + k^2(\chi(\mathbf{x}) + 1)u_j(\mathbf{x}) = 0, \quad \mathbf{x} \in \mathbb{R}^d, \quad (2.1)$$

where k is the wavenumber of the homogeneous background media. The total field u_j can be represented by the intergral equation [6],

$$u_j(\mathbf{x}) = u_j^{inc}(\mathbf{x}) + k^2 \int_{\Omega} g(\mathbf{x}, \mathbf{x}') \chi(\mathbf{x}') u_j(\mathbf{x}') dv(\mathbf{x}'), \quad (2.2)$$

where $g(\mathbf{x}, \mathbf{x}')$ is the Green's function of the homogeneous background medium:

$$g(\mathbf{x}, \mathbf{x}') = \begin{cases} \frac{i}{4} H_0^{(1)}(k|\mathbf{x} - \mathbf{x}'|) & \text{for } d = 2, \\ \frac{e^{ik|\mathbf{x} - \mathbf{x}'|}}{4\pi|\mathbf{x} - \mathbf{x}'|} & \text{for } d = 3 \end{cases}$$

where $H_0^{(1)}$ is the zero-order Hankel function of first kind. We note that the total field u may stand for the acoustic pressure in an acoustic scattering problem, or for the electric

field vector in an electromagnetic scattering, or for the particle-velocity vector in an elastodynamic scattering. The scattered field is measured on the boundary of a domain S , which is sitting outside the scatterer Ω . As the scatterer Ω is unknown, we shall introduce a sampling domain \mathbf{D} that completely cover the scatterer Ω . As the contrast function χ vanishes outside Ω , with the help of (2.2) we can write the scattered field as

$$u_j^{sca}(\mathbf{x}) = u_j(\mathbf{x}) - u_j^{inc}(\mathbf{x}) = k^2 \int_{\mathbf{D}} g(\mathbf{x}, \mathbf{x}') \chi(\mathbf{x}') u_j(\mathbf{x}') dv(\mathbf{x}'), \quad \mathbf{x} \in S. \quad (2.3)$$

For sake of convenience, we shall often introduce the contrast source function

$$w_j(\mathbf{x}) = \chi(\mathbf{x}) u_j(\mathbf{x}), \quad \mathbf{x} \in \mathbf{D}. \quad (2.4)$$

Then we can write (2.2) and (2.3) in the following more compact forms

$$w_j(\mathbf{x}) = \chi(\mathbf{x}) u_j^{inc}(\mathbf{x}) + \chi(\mathbf{x}) (G_D w_j)(\mathbf{x}), \quad \mathbf{x} \in \mathbf{D}, \quad (2.5)$$

and

$$u_j^{sca}(\mathbf{x}) = (G_S w_j)(\mathbf{x}), \quad \mathbf{x} \in S, \quad (2.6)$$

where G_D and G_S are two integral operators given by

$$\begin{aligned} (G_D w)(\mathbf{x}) &= k^2 \int_{\mathbf{D}} g(\mathbf{x}, \mathbf{x}') w(\mathbf{x}') dv(\mathbf{x}') \quad \forall \mathbf{x} \in \mathbf{D}, \\ (G_S w)(\mathbf{x}) &= k^2 \int_{\mathbf{D}} g(\mathbf{x}, \mathbf{x}') w(\mathbf{x}') dv(\mathbf{x}') \quad \forall \mathbf{x} \in S. \end{aligned}$$

Equations (2.5) and (2.6) will be two fundamental equations for our proposed multilevel initialization algorithm.

3 Approximate contrast source by backpropagation

We can easily see that the support of the contrast source function $w = \chi u$ describes the exact locations and geometries of all the inhomogeneous media, which generate a scattered field u^{sca} . The aim of this work is to propose a fast and less expensive algorithm that can help locate all the inhomogeneous media and provide good initial guesses for some computationally more demanding iterative algorithms to find more accurate approximations of the contrast function χ .

Our algorithm will rely on the approximate contrast source obtained by backpropagation. Backpropagation is widely used in inverse medium scatterings, see [17] [10] and the references therein. In this section we shall give a rigorous mathematical explanation of the approximate contrast source by backpropagation. Let $(\cdot, \cdot)_{L^2(S)}$ and $(\cdot, \cdot)_{L^2(D)}$ be the scalar products respectively in $L^2(S)$ and $L^2(D)$, and $G_s^*: L^2(S) \rightarrow L^2(D)$ be the adjoint of operator $G_s: L^2(D) \rightarrow L^2(S)$. G_s^* is called the backpropagation operator and given by

$$(G_s^* w)(\mathbf{x}) = k^2 \int_S \overline{g(\mathbf{x}, \mathbf{x}')} w(\mathbf{x}') ds(\mathbf{x}') \quad \forall \mathbf{x} \in \mathbf{D}.$$

We shall need the following backpropagation subspace of $L^2(D)$,

$$V_b = \text{span} \{G_s^* u^{sca}\},$$

which is formed by all the fields generated by the backpropagation G_s^* on the scattered data u^{sca} . It follows from (2.6) that

$$u^{sca}(\mathbf{x}) = (G_S w)(\mathbf{x}), \quad \mathbf{x} \in S. \quad (3.1)$$

The backpropagation is to seek a best approximate solution w_b to the equation (3.1) in the backpropagation subspace V_b , namely

$$\|u^{sca} - G_s w_b\|_{L^2(S)}^2 = \min_{v_b \in V_b} \|u^{sca} - G_s v_b\|_{L^2(S)}^2. \quad (3.2)$$

It is easy to see that the solution w_b to (3.2) solves the variational system:

$$(u^{sca} - G_s w_b, G_s v_b)_{L^2(S)} = 0 \quad \forall v_b \in V_b, \quad (3.3)$$

or equivalently,

$$(G_s w_b, G_s v_b)_{L^2(S)} = (G_s^* u^{sca}, v_b)_{L^2(D)} \quad \forall v_b \in V_b. \quad (3.4)$$

As $w_b, v_b \in V_b$, we can write

$$w_b = \lambda G_s^* u^{sca}, \quad v_b = \mu G_s^* u^{sca} \quad (3.5)$$

for some constants λ, μ . Substituting the two expressions into (3.4) we obtain

$$\lambda = \frac{\|G_s^* u^{sca}\|_{L^2(D)}^2}{\|G_s G_s^* u^{sca}\|_{L^2(S)}^2}, \quad (3.6)$$

which gives the approximate contrast source by backpropagation:

$$w_b = \frac{\|G_s^* u^{sca}\|_{L^2(D)}^2}{\|G_s G_s^* u^{sca}\|_{L^2(S)}^2} G_s^* u^{sca}. \quad (3.7)$$

4 A multilevel algorithm

In this section we propose a fast multilevel algorithm to find the locations and geometries of all the inhomogeneous media, which are described by the contrast function χ in (2.1). The algorithm proceeds iteratively, and carries out two important steps at each iteration based on the two fundamental equations (2.5) and (2.6), namely the state and field equations. In the first step, we apply the backpropagation technique to compute an approximate contrast source w_j corresponding to each incident u_j^{inc} ($j = 1, 2, \dots, N_i$). It follows from (3.7) that this approximation is given by

$$w_j = \frac{\|G_S^* u_j^{sca}\|_{L^2(D)}^2}{\|G_S G_S^* u_j^{sca}\|_{L^2(S)}^2} G_S^* u_j^{sca}, \quad j = 1, 2, \dots, N_i. \quad (4.1)$$

With these approximate contributions w_j of the exact contrast source w corresponding to each incident u_j^{inc} , we approximate the contrast χ pointwise by minimizing the residual equation corresponding to the state equation (2.5), namely

$$\min_{\chi(\mathbf{x}) \in \mathbf{R}^1} \sum_{j=1}^{N_i} \left| (\chi u_j^{inc} - w_j + \chi G_D w_j)(\mathbf{x}) \right|^2, \quad (4.2)$$

which yields an explicit formula to compute an approximate contrast value $\chi(\mathbf{x})$ at every point $\mathbf{x} \in D$ when an approximate contrast source w_j is available:

$$\chi(\mathbf{x}) = \frac{\sum_{j=1}^{N_i} w_j(\mathbf{x}) \overline{(u_j^{inc} + G_D w_j)(\mathbf{x})}}{\sum_{j=1}^{N_i} |(u_j^{inc} + G_D w_j)(\mathbf{x})|^2}, \quad (4.3)$$

where the overbar denotes the complex conjugate.

Clearly both (4.1) and (4.3) are rather crude mostly, and may provide rather poor approximations for the exact contrast source w and contrast profile χ . But as it will be seen, when we combine these two poor approximations in a novel manner with some multilevel technique, it generates a very efficient and robust algorithm for locating an accurate position and shape of each inhomogeneous medium.

Our basic idea is also based on another simple observation. We know that the exact contrast function $\chi(\mathbf{x})$ vanishes outside the scatterer Ω , so its support provides the location and shape of the scatterer Ω , which is formed by all the inhomogeneous media. This observation, along with the previous two explicit evaluation formulae (4.1) and (4.3) and a novel multilevel technique, forms the foundation of our new multilevel sampling algorithm.

For the description of the algorithm, we first introduce two new concepts, *the smallest distance* and *the first gap interval* with index M . For a given finite positive sequence, $\{a_1, a_2, \dots, a_m\}$, *its smallest distance* is the positive smallest one among all the distances between two neighboring elements, namely $dist(a_i, a_{i+1})$, $i = 1, 2, \dots, m - 1$. Among all these $m - 1$ distances, if there exists some j such that $2 \leq j \leq m - 1$ and the distance $dist(a_j, a_{j+1})$ is M times larger than *the smallest distance* of the sequence $\{a_1, a_2, \dots, a_j\}$, then $[a_j, a_{j+1}]$ is called *a gap interval*. The first such interval is called *the first gap interval*.

Now we are ready to state our new algorithm.

Multilevel Sampling Algorithm.

1. Choose a sampling domain \mathbf{D} that contains the scatterer Ω ;
 Select a uniform (coarse) mesh on \mathbf{D} , consisting of rectangular (2D) or cubic (3D) elements; write the mesh as D_1 ;
 Select a tolerance ε and an index M ; set an initial cut-off value $c_0 := 0$ and $k := 1$.
2. Compute an approximate value of the contrast $\chi_k(\mathbf{x})$ at each grid point $\mathbf{x} \in D_k$, using the formulae (4.1) and (4.3). Then do the following:

- 2.1 Order all the values of $\chi_k(\mathbf{x})$ satisfying $\chi_k(\mathbf{x}) \geq c_{k-1}$ into a non-decreasing sequence;
Find *the first gap interval* of the sequence with index M ;
Choose the right endpoint of *this first gap interval* as the next cut-off value c_k .
- 2.2 If $\chi_k(\mathbf{x}) \geq c_k$ at a grid point \mathbf{x} , select all the grid points of the elements which share \mathbf{x} as one of its vertices;
Remove all the grid points in D_k , which are not selected;
Update D_k by all those selected grid points.
3. If $|c_k - c_{k-1}| \leq \varepsilon$, go to Step 4;
otherwise refine the mesh D_k to get D_{k+1} ; set $k := k + 1$ and go to Step 2.
4. Output all grid points in D_k for the supports of all inhomogeneous media;
Output the approximate contrast values $\chi_k(\mathbf{x})$ at all grid points of D_k .

We can easily see that the Multilevel Sampling Algorithm does not involve any optimization process or matrix inversions, and its major cost is to update the contrast values using the explicit formulae (4.1) and (4.3) at each iteration, and the computational sampling domain D_k shrinks as the iteration goes. So the algorithm is rather simple and less expensive. In addition, as the cut-off values are basically to distinguish the homogeneous background medium where $\chi(\mathbf{x})$ vanishes and the inhomogeneous media where $\chi(\mathbf{x})$ should be essentially different from 0, so our cut-off values are rather easy to choose and insensitive to the size and physical features of scatterers. In fact, the cut-off value can start simply with zero, then it is updated automatically with the iteration. As we shall see from numerical examples in the next section, the algorithm works well with few incidents, even with one; and it is self-adaptive, namely it can recover some elements that have been removed at the previous iterations due to the computational errors. In terms of these aspects the new Multilevel Sampling Algorithm outperforms the popular linear sampling methods [15], including the improved multilevel variant [11].

Discretization. We end this section with a brief discussion about numerical discretization of the integrations involved in the above multilevel algorithm. We illustrate only the discretization of (2.5) and (2.6), as all other integrations involved in the algorithm can be approximated similarly. To do so, we divide the domain \mathbf{D} into smaller rectangular or cubic elements, whose centers are denoted as $\mathbf{x}_1, \mathbf{x}_2, \dots, \mathbf{x}_M$. Using the coupled-dipole method (CDM) or discrete dipole approximation (DDA) [3, 9], we can discretize (2.5) by

$$w_j(\mathbf{x}_m) = \chi(\mathbf{x}_m)u_j^{inc}(\mathbf{x}_m) + k^2\chi(\mathbf{x}_m) \sum_{n \neq m} A_n g(\mathbf{x}_m, \mathbf{x}_n) w_j(\mathbf{x}_n), \quad m = 1, 2, \dots, M, \quad (4.4)$$

where A_n is the area or volume of the n -th element. Similarly, we can discretize equation (2.6) at every point $\mathbf{x} \in \mathbf{S}$ by

$$u_j^{sca}(\mathbf{x}) = k^2 \sum_{n=1}^M A_n g(\mathbf{x}, \mathbf{x}_n) w_j(\mathbf{x}_n) \quad \text{for } j = 1, 2, \dots, N_i. \quad (4.5)$$

5 Numerical simulations

In this section we present several examples to test the effectiveness of our multilevel sampling algorithm. We first list the parameters that are used in our numerical simulations: the wave number k and wave length λ are taken to be $k = 2\pi$ and $\lambda = 1$; the number of incidences and receivers are set to be $N_i = 6$ and $N_s = 30$ respectively, both equally distributed on the circle of radius 5λ ; the index M of the first gap interval and the tolerance parameter ε are chosen to be 100 and 10^{-3} respectively. In all the numerical simulations, random noises are added to the exact scattering data in the following form:

$$u_j^{sca}(\mathbf{x}) := u_j^{sca}(\mathbf{x})[1 + \xi(r_{1,j}(\mathbf{x}) + ir_{2,j}(\mathbf{x}))], \quad j = 1, 2, \dots, N_i$$

where $r_{1,j}(\mathbf{x})$ and $r_{2,j}(\mathbf{x})$ are two random numbers varying between -1 and 1, and ξ corresponds to the level of the noise, which is usually taken to be 10% unless specified otherwise. All the programs in our experiments are written in MATLAB and run on a 2.83GHz PC with 4GB memory.

5.1 Two-dimensional reconstructions

Example 1. This example shows a scatterer Ω consisting of two squares of side length 0.3λ , located respectively at $(-0.3\lambda, -0.3\lambda)$ and $(0.3\lambda, 0.3\lambda)$, with their contrast values being 1 and 2 respectively; see the two red squares in Figure 2(a). We take the sampling domain $\mathbf{D} = [-1.2\lambda, 1.2\lambda] \times [-1.2\lambda, 1.2\lambda]$, which is quite large compared to the scatterer Ω , with its area of 64 times of the area of one scatterer component. More importantly, we see that these two small objects are quite close to each other. The mesh refinement during the multilevel algorithm is carried out based on the rule $h_k = 0.4\lambda/2^k$, where k is the k -th refinement, and h_0 and h_k are respectively the mesh sizes of the initial mesh and the mesh after the k th refinement. The numerical reconstructions are shown in Figure 2(b) - 2(d) respectively for the 1st, 3rd and 5th iteration. One can observe from the figures that the algorithm converges very fast and provides accurate locations of the two medium components in only 5 iterations. Moreover, we can see an important advantage of the algorithm, i.e., it can separate the disjoint medium components quickly.

Example 2. This example is the same as Example 1, except that the contrast values of two medium components are now variable functions, namely

$$\chi(x, y) = \sin \frac{\pi(10|x| - 1.5)}{3} \sin \frac{\pi(10|y| - 1.5)}{3}.$$

The numerical reconstructions are shown in Figure 3(b)- 3(d) for the 1st, 3rd and 6th iteration. Again, we observe from the figures that the algorithm converges fast, provides very satisfactory locations of the two medium components in only 6 iterations, and it can separate the disjoint medium components quickly.

Example 3. This example considers a scatterer Ω of a thin annulus with the inner and outer radii being 0.3λ and 0.5λ respectively and centered at the origin. The contrast

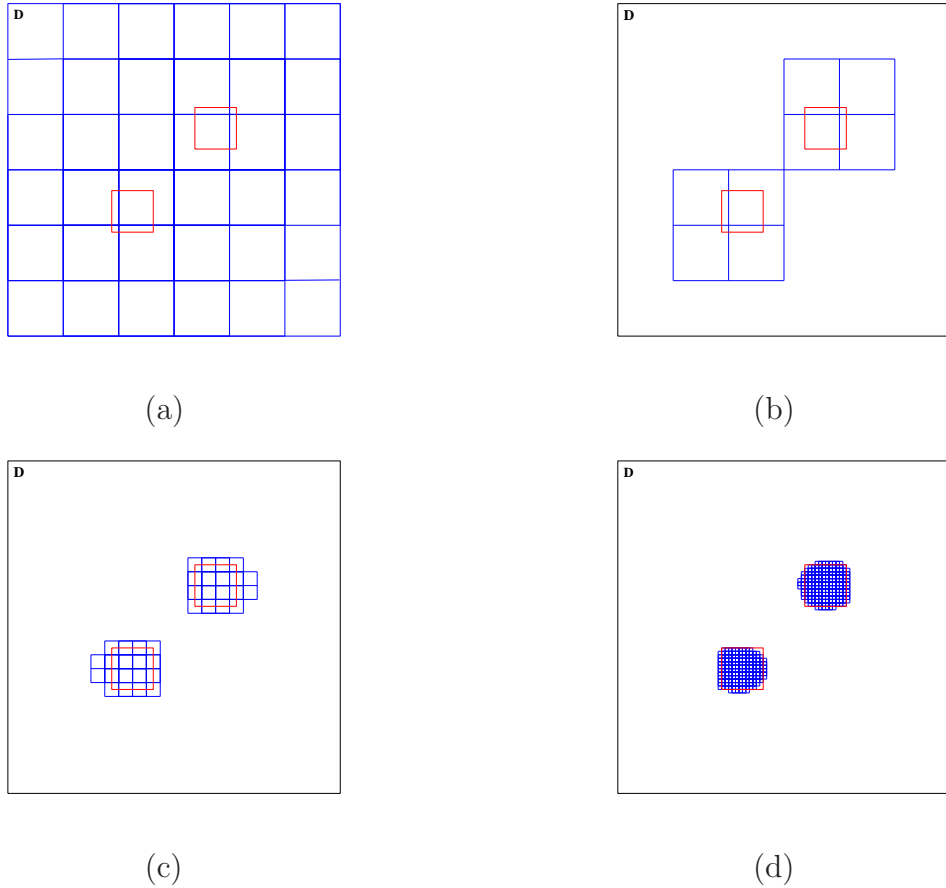


Figure 2: (a) The initial (coarse) mesh on the sampling domain; (b)-(d) Reconstructions at the 1st, 3rd and 5th iteration.

value $\chi(\mathbf{x})$ is 2 inside the thin annulus. The sampling domain \mathbf{D} is taken to be a square of side length with 5.6λ , as shown in Figure 4(a).

It is easy to see the sampling domain \mathbf{D} has an area of about 62 times as large as the one of the annulus, and the annulus has a very thin thickness, i.e., 0.2λ . The mesh refinement during the multilevel algorithm is carried out based on the rule $h_k = 0.4\lambda/2^k$, where k indicates the k -th refinement and h_k is the mesh size after the k th refinement. The numerical reconstructions are shown in Figure 4(b)- 4(d) for the 1st, 3rd and 4th iteration. Same as for the previous two examples, the reconstructions are quite satisfactory and the accurate locations of the scatterer can be achieved.

5.2 Reconstruction for the contrast function χ

There are many numerical reconstruction methods available in the literature for the contrast profile function χ , that are robust and more accurate than our new multilevel method. But these methods are usually more complicated technically and much more

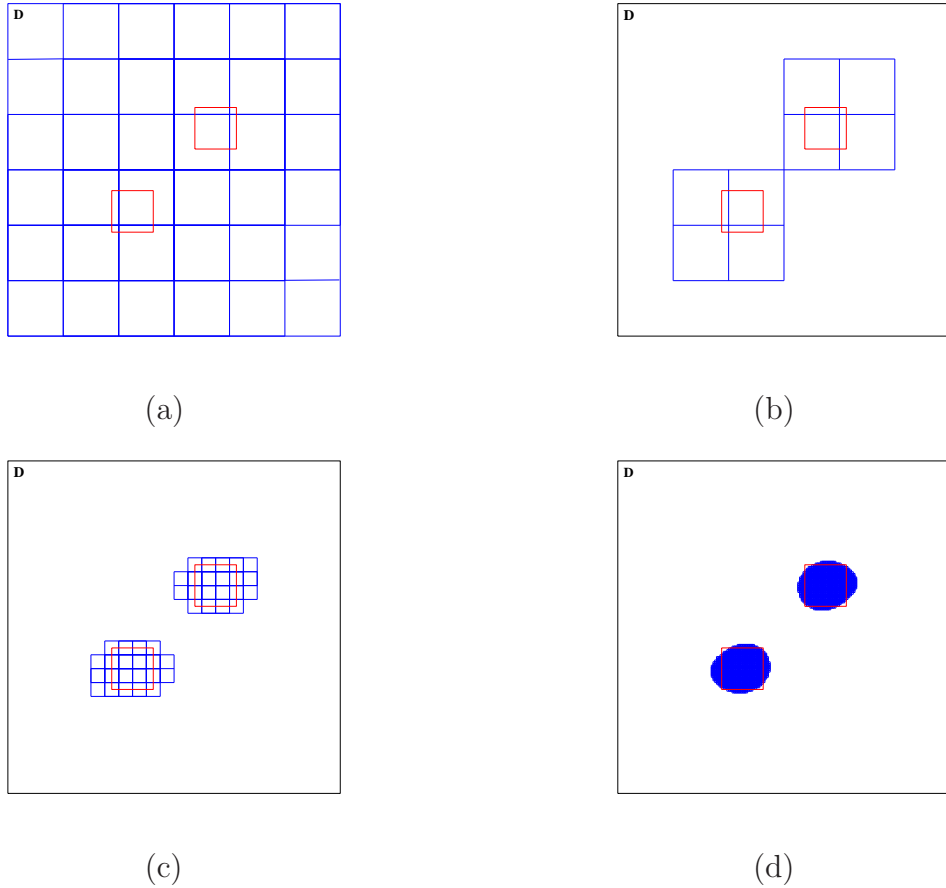


Figure 3: (a) The first coarse mesh on the sampling region; (b)-(d) Reconstructions at the 1st, 3rd and 6th iteration.

demanding computationally, as they mostly involve nonlinear optimizations and matrix inversions. Without a reasonably good initial location for each inhomogeneous medium, we may have to take a much larger sampling domain than required so these methods can be extremely time consuming, especially in three dimensions. Using the newly proposed multilevel algorithm in Section 4, we can first locate a much smaller sampling domain than usual (or the one we originally selected) in a numerical reconstruction for the contrast χ . Then we can apply any existing reconstruction algorithms for more accurate reconstructions, starting with an initial sampling domain provided by the new multilevel algorithm. This may save us a great fraction of the entire computational costs.

Next we show numerical tests by combining our new multilevel method with the popular extended contrast source inversion (ECSI) method [17]. Firstly, we consider the same scatterer Ω and the set-ups as in Example 1 of Section 5.1; see Figure 5(a). Then we apply the ECSI method [17] with mesh size $h = 0.01\lambda$ to the reconstructed domain (cf. Figure 2(d)) by the multilevel algorithm. The reconstruction result is shown in Figure 5(b). Clearly, one can see that both the location and the values of the contrast

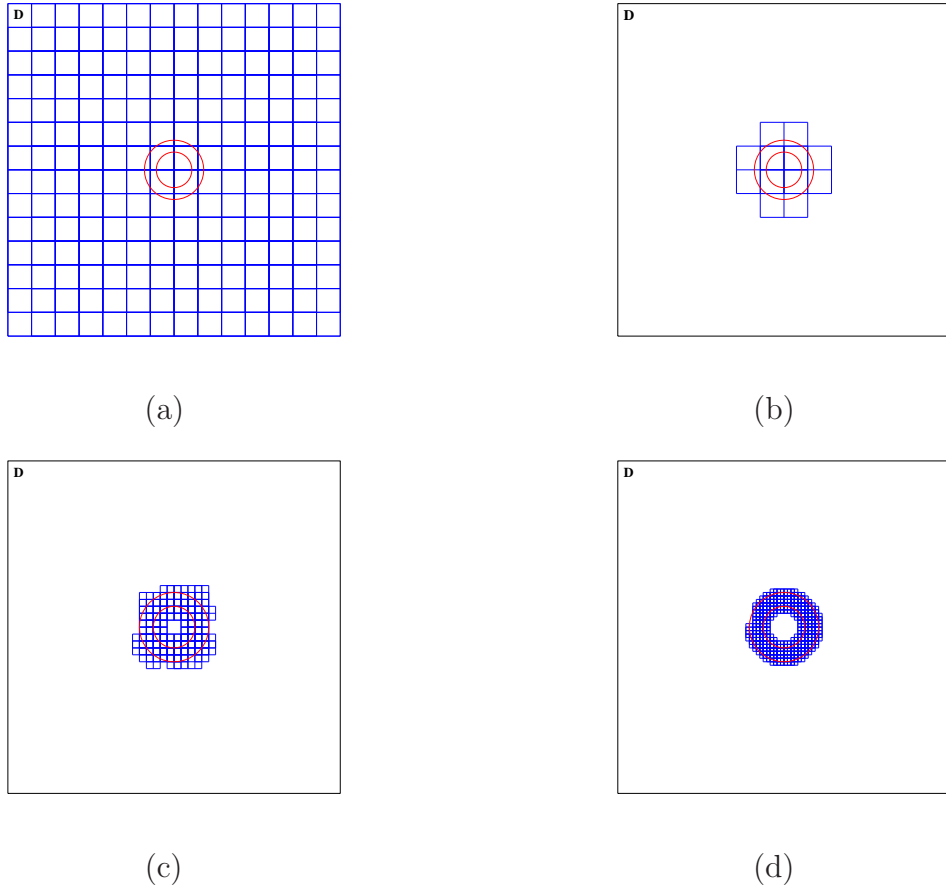


Figure 4: (a) The first coarse mesh on the sampling region; (b)-(d) Reconstructions at the 1st, 3rd and 4th iteration.

are well reconstructed.

Secondly, we consider the same scatterer Ω and the set-ups as in Example 3 of Section 5.1; see Figure (5)(c). We apply the ECSI method [17] with mesh size $h = 0.025\lambda$ to the reconstructed domain (cf. Figure 4(d)) obtained by the multilevel algorithm. The reconstruction result is shown in Figure 5(d). Clearly, both of the location and the values of the contrast are well reconstructed.

5.3 Three-dimensional reconstructions

Example 4. This example tests a three-dimensional scatterer Ω consisting of two small cubic components:

$$\Omega_1 = [-0.45\lambda, -0.15\lambda]^3, \quad \Omega_2 = [0.15\lambda, 0.45\lambda]^3.$$

The two squares are quite close to each other, both with constant contrast values 2; see Figure 6(a). We take the sampling domain to be $\mathbf{D} = [-1.2\lambda, 1.2\lambda]^3$, which is about 500 times of the volume of Ω_1 or Ω_2 .

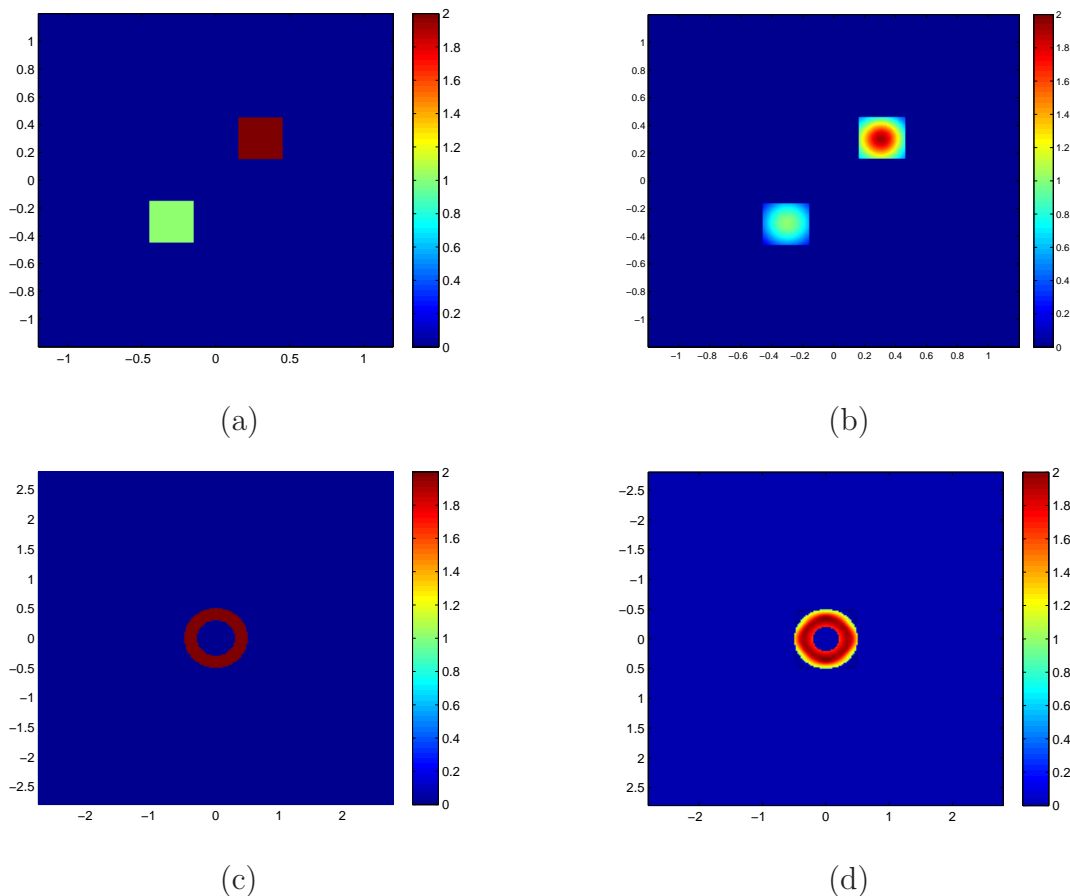


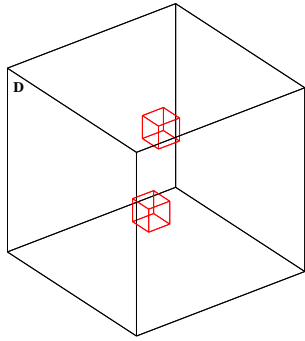
Figure 5: (a) True scatterer in Example 1; (b) Reconstruction by combining the multilevel method with ECSI for Example 1; (c) True scatterer in Example 3; (d) Reconstruction by combining the multilevel method with ECSI for Example 3

We take an initial mesh size of $h_0 = 0.8\lambda$ in the multilevel algorithm. The mesh refinement during the multilevel algorithm is carried out based on the rule $h_k = 0.8\lambda/2^k$, where k is the k -th refinement, and h_k is the mesh size after the k th refinement. The numerical reconstructions are shown in Figure 7. Same as for the previous two-dimensional examples, the reconstructions are quite satisfactory and the accurate locations of the scatterer can be achieved, and two inhomogeneous medium objects can be quickly separated.

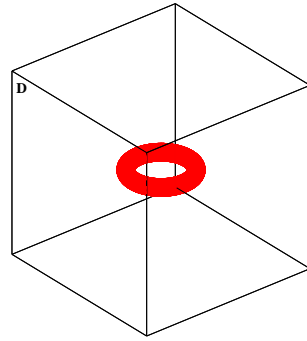
Example 5. In this test we consider a torus scatterer (see Figure 6(b)), with a contrast value 2. The torus has the following representation,

$$\left(R - \sqrt{x^2 + y^2}\right)^2 + z^2 = r^2,$$

where $r = 0.1\lambda$ and $R = 0.4\lambda$ (R is the radius from the center of the hole to the center of the torus tube, r is the radius of the tube). The sampling domain is taken to be $\mathbf{D} = [-1.2\lambda, 1.2\lambda]^3$, which is about 170 times of the volume of the torus.

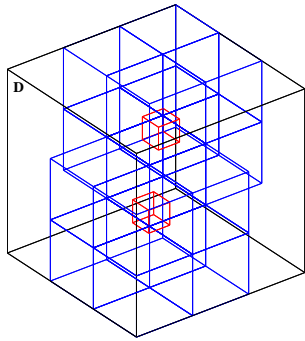


(a)

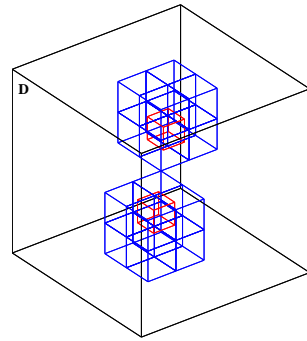


(b)

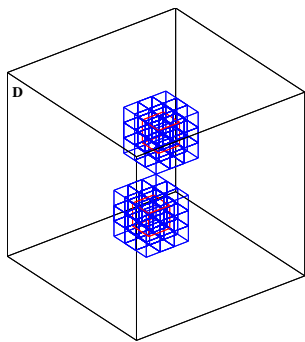
Figure 6: Scatterers imbedded in a large sampling domain: two cubic components close to each other (a); a torus (b)



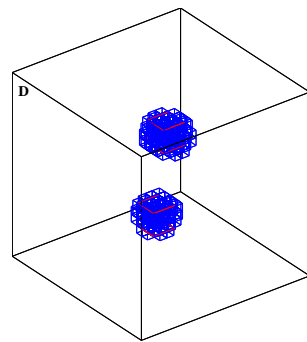
(a)



(b)



(c)



(d)

Figure 7: Numerical reconstructions by the first 4 iterations

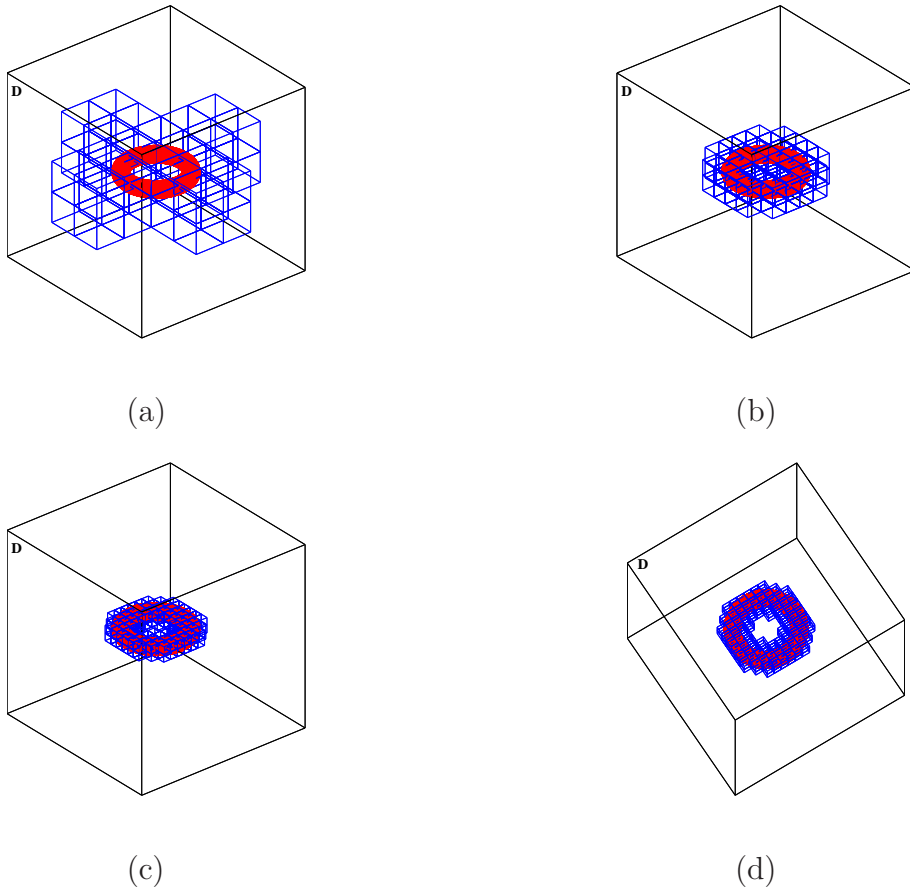


Figure 8: *Numerical reconstructions by the first 3 iterations; (d) is the same as (c), but viewed in a different angle.*

We take an initial mesh size of $h_0 = 0.4\lambda$ in the multilevel algorithm. The mesh refinement during the multilevel algorithm is carried out based on the rule $h_k = 0.4\lambda/2^k$, where k is the k -th refinement, and h_k is the mesh size after the k th refinement. The numerical reconstructions are shown in Figure 8. Same as for the previous two-dimensional examples, the reconstructions are quite satisfactory and the accurate locations of the scatterer can be achieved.

6 Concluding remarks

This work proposes a multilevel sampling algorithm which helps locate an initial computational domain for the numerical reconstruction of inhomogeneous media in inverse medium scatterings. The algorithm is an iterative process which starts with a large sampling domain, and reduces the size of the domain iteratively based on the cut-off values, which are computed adaptively by using the updated contrast source strengths and contrast values at each iteration. The iterative algorithm can be viewed actually as a direct

method, since it involves only matrix-vector operations and does not need any optimization process or to solve any large-scale ill-posed linear systems. The algorithm works with very few incident fields and its cut-off values are easy to compute and insensitive to the sizes and shapes of the scatterers, as well as the noise in the data. This is a clear advantage of the algorithm over some popular existing sampling methods such as the linear sampling type methods, where the cut-off values are sensitive to the noise and difficult to choose, and the number of incident fields can not be small. In addition, the multilevel algorithm converges fast and can easily separate multiple disjoint scattering components, often with just a few iterations to find a satisfactory initial location of each object. Another nice feature of the new algorithm is that it is self-adaptive, that is, it can remedy the possible errors from the previous levels at each current level. With an effective initial location of each object, we may then apply any existing efficient but computationally more demanding methods for further refinement of the estimated shape of each scattering object as well as for recovery of the contrast profiles of different media.

References

- [1] A. Abubakar and P. M. van den Berg, The contrast source inversion method for location and shape reconstructions, *Inverse Problems* **18** (2002), pp.495-510.
- [2] G. Bao and P. Li, Inverse medium scattering for the Helmholtz equation at fixed frequency, *Inverse Problems* **21** (2005), pp.1621-1641.
- [3] K. Belkebir, P. C. Chaumet and A. Sentenac, Superresolution in total internal reflection tomography, *J. Opt. Soc. Amer. A* **22** (2005), pp.1889-1897.
- [4] X. Chen, Application of signal-subspace and optimization methods in reconstructing extended scatterers, *J. Opt. Soc. Amer. A* **26** (2009), pp.1022-1026.
- [5] X. Chen, Subspace-based optimization method for solving inverse-scattering problems, *IEEE Trans. Geosci. Remote Sensing* **48** (2010), pp.42-49.
- [6] D. Colton and R. Kress, *Inverse Acoustic and Electromagnetic Scattering Theory*, 2nd ed., Springer Verlag, Berlin, 1998.
- [7] K. Ito, B. Jin and J. Zou, A direct sampling method to an inverse medium scattering problem, *Inverse Problems* **28** (2012), 025003 (11pp).
- [8] A. Kirsch, The MUSIC-algorithm and the factorization method in inverse scattering theory for inhomogeneous media, *Inverse Problems* **18** (2002), pp.1025-1040.
- [9] A. Lakhtakia, Strong and weak forms of the method of moments and the coupled dipole method for scattering of time-harmonic electromagnetic fields, *Int. J. Modern Phys. C* **3** (1992), pp.583-603.

- [10] B. Levy and C. Esmersoy, Variable background Born inversion by wavefield back-propagation, *SIAM J. Appl. Math.* **48** (1988), pp. 952-972.
- [11] J. Li, H. Liu and J. Zou, Multilevel linear sampling method for inverse scattering problems, *SIAM J. Sci. Comp.* **30** (2008), pp. 1228-1250.
- [12] J. Li, H. Liu and J. Zou, Strengthened linear sampling method with a reference ball, *SIAM J. Sci. Comp.* **31** (2009), pp. 4013-4040.
- [13] K. Liu, Y. Xu and J. Zou, A parallel radial bisection algorithm for inverse scattering problems, *Inv. Prob. Sci. Eng.* (2012), pp. 1-13.
- [14] E. A. Marengo, F. K. Gruber and F. Simonetti, Time-reversal MUSIC imaging of extended targets, *IEEE Trans. Image Proc.* **16** (2007), pp. 1967-1984.
- [15] R. Potthast, A survey on sampling and probe methods for inverse problems, *Inverse Problems* **22** (2006), pp. R1-R47.
- [16] P. M. van den Berg and R. E. Kleinman, A contrast source inversion method, *Inverse Problems* **13** (1997), pp. 1607-1620.
- [17] P. M. van den Berg, A. L. van Broekhoven and A. Abubakar, Extended contrast source inversion, *Inverse Problems* **15** (1999), pp. 1325-1344.